Proton structure, muon-proton interactions and the proton radius puzzle

RICHARD HILL

THE UNIVERSITY OF CHICAGO

Project X workshop
20 June 2012

Based on work w/ G. Paz, Phys.Rev.Lett. 107 (2011) 160402, Phys.Rev. D82 (2010) 113005

the proton radius puzzle

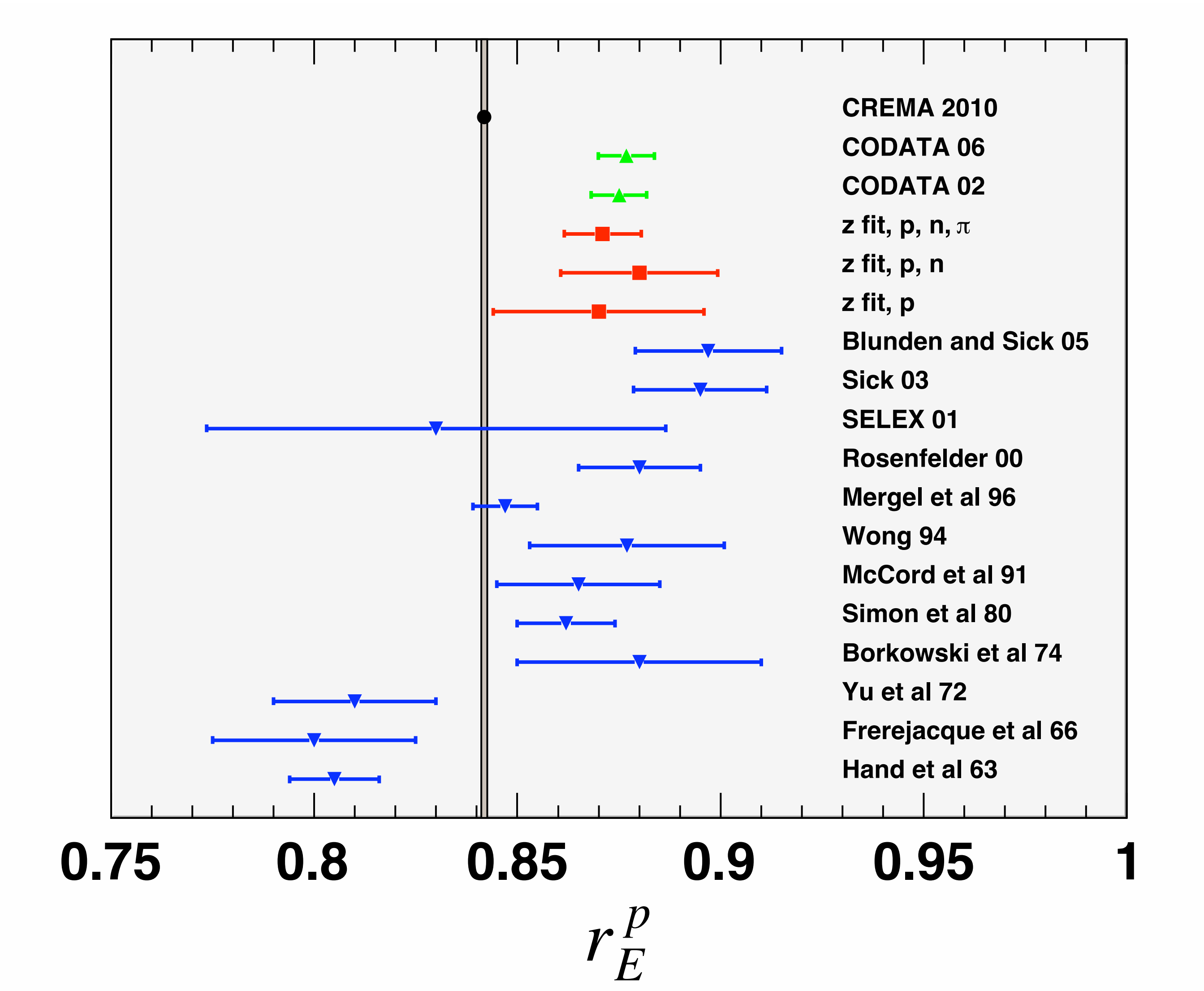

- inferred from muonic H

- inferred from electronic H

- extraction from e p, e n scattering, ππNN data (this talk)

- previous extractions from e p scattering (as tabulated in PDG)

This talk:

- formalism for proton/nuclear structure effects in hydrogenic bound states
- analyticity and nucleon form factors
- status of the proton radius puzzle(s)

comparison of muon anomalies:

	$(g-2)_\mu$	r_E^p
significance	3.6σ e+e- 2.4σ τ	5σ H spectroscopy 1σ - 5σ ep scattering
hadronic uncertainties	hadronic vac. pol, light-by-light	charge radius, two-photon exchange
new physics/SUSY interpretation	≈✓ ?	?

A basic problem in the measurement of fundamental parameters (or new physics?)

A thorny (fun) problem at the interfaces of atomic, nuclear and particle physics.

"Data from muonic hydrogen are **so inconsistent with the other data that they have not been included** in the determination of r_p and thus do not have an influence on R_∞" - CODATA 2010

"Until the difference between the *e p* and *μ p* values is understood, it does not make much sense to average all the values together. For the present, we stick with the less precise (and provisionally suspect) CODATA 2006 value. **It is up to workers in this field to solve this puzzle**." - PDG 2011

"Testing of this result is **among the most timely and important measurements in physics**" - JLab PAC, 2011

significant interest from multiple perspectives

aside: proton axial radius puzzle

Charged current quasielastic scattering:
basic signal process for neutrino oscillation

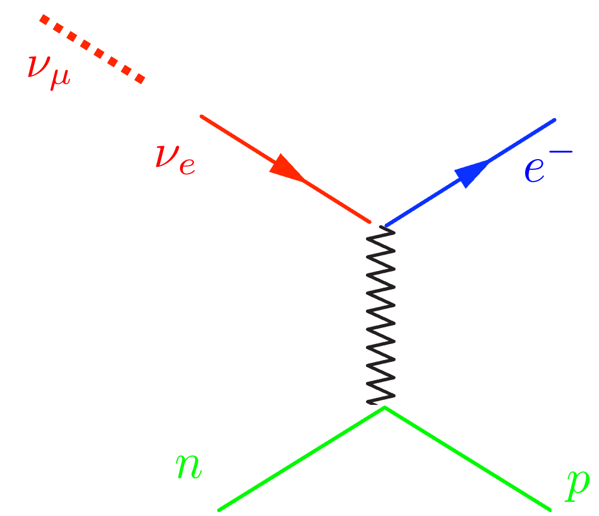

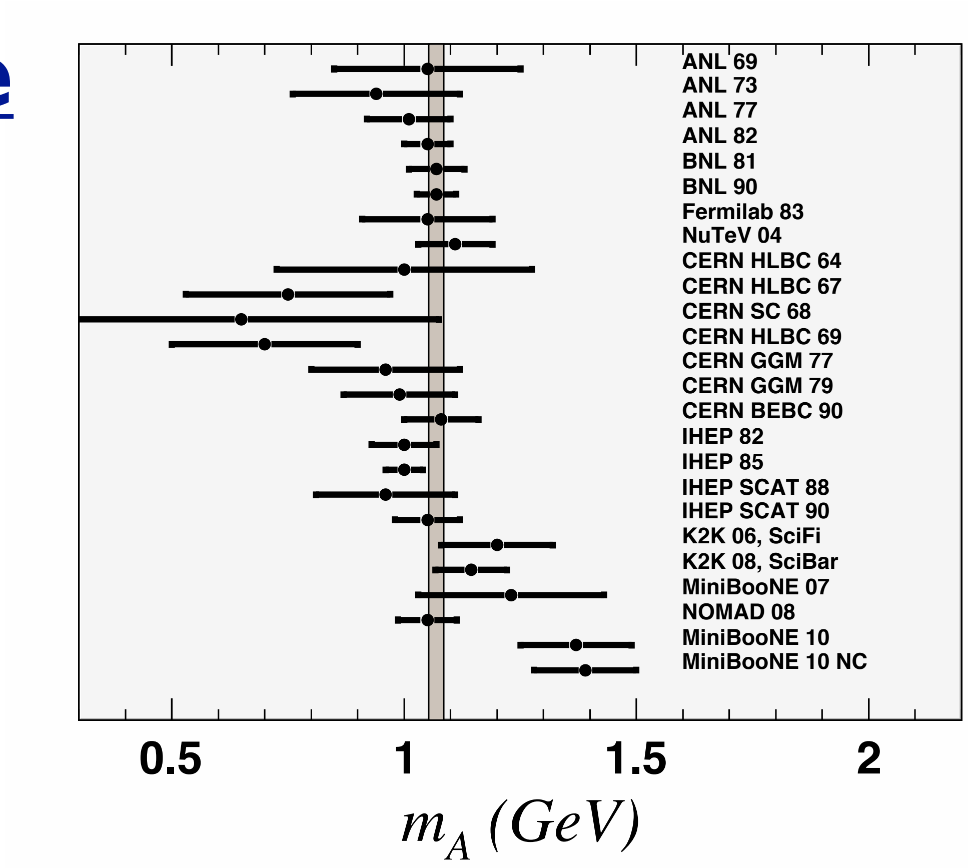

$$\langle p(p')|J_W^{+\mu}|n(p)\rangle \propto \bar{u}^{(p)}(p')\Big\{\gamma^\mu F_1(q^2) + \frac{i}{2m_N}\sigma^{\mu\nu}q_\nu F_2(q^2)$$

$$+\gamma^\mu\boxed{\gamma_5 F_A(q^2)} + \frac{1}{m_N}q^\mu\gamma_5 F_P(q^2)\Big\}u^{(n)}($$

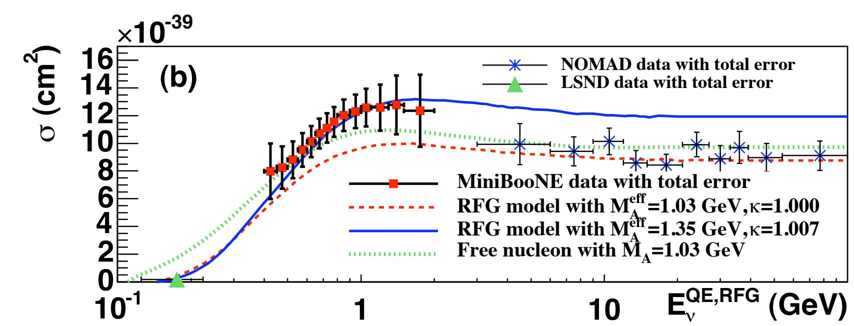

Considerable uncertainty and discrepancies in cross section from

- axial-vector form factor
- nuclear effects

$$F_A^{\rm dipole}(q^2) = \frac{F_A(0)}{\left[1 - q^2/(m_A^{\rm dipole})^2\right]^2}\,, \qquad m_A \equiv \sqrt{\frac{2F_A(0)}{F_A'(0)}}$$

Both are essential to the interpretation of neutrino oscillation studies

progress in theoretical tools:

- z expansion and dispersive analysis
  - free gift from field theory to analyze scattering data
  - wide range of applications: EM form factors, neutrino scattering, meson transitions, ...
- high orders of NRQED
  - define the charge radius and other proton structure corrections in presence of radiative corrections
  - model independent spectroscopic predictions in terms of scattering data

NRQED and proton structure

energy, momenta << M: integrate out M

[Caswell, Lepage 1986]

μ_p $\qquad\qquad$ r_E^p

$$
\begin{aligned}
\mathcal{L}_{\mathrm{NRQED}} = \psi_p^\dagger \Big\{ & iD_t + \frac{\boldsymbol{D}^2}{2m_p} + \frac{\boldsymbol{D}^4}{8m_p^3} + \dots + c_F \frac{e\boldsymbol{\sigma}\cdot\boldsymbol{B}}{2m_p} + c_D \frac{e(\boldsymbol{D}\cdot\boldsymbol{E} - \boldsymbol{E}\cdot\boldsymbol{D})}{8m_p^2} + c_S \frac{ie\boldsymbol{\sigma}\cdot(\boldsymbol{D}\times\boldsymbol{E} - \boldsymbol{E}\times\boldsymbol{D})}{8m_p^2} \\
& + c_{A1} e^2 \frac{\boldsymbol{B}^2 - \boldsymbol{E}^2}{8m_p^3} - c_{A2} e^2 \frac{\boldsymbol{E}^2}{16m_p^3} + \dots \Big\} \psi_p + \psi_\mu^\dagger \{ iD_t + \dots \} \psi_\mu + \frac{d_2}{m_\mu m_p} \psi_p^\dagger \psi_p \psi_\mu^\dagger \psi_\mu + \dots
\end{aligned}
$$

$\bar{\alpha},\ \bar{\beta}$ $\qquad\qquad$ $?$

proton structure appears as non-pointlike values for Wilson coefficients

- matching performed by computation, or comparison to experiment

- relativistic invariance (infinite dimensional realization of Poincare) implies constraints on coefficients: $c_S = 2\,c_F - 1$, etc.

- muonic hydrogen Lamb shift: need c_D through $O(\alpha)$, d_2 through $O(\alpha^2)$

NRQED part (I): vertex corrections

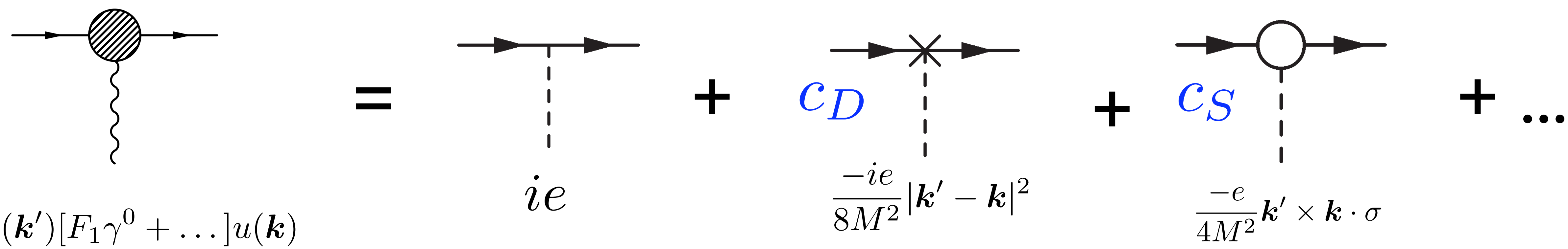

$$\langle k'|J^{\mu}_{\rm e.m.}|k\rangle = \bar{u}(k')\left[\gamma^\mu F_1(q^2) + \frac{i}{2M}F_2(q^2)\sigma^{\mu\nu}q_\nu\right]u(k)$$

Convenient to work in terms of Sachs basis:

$$\begin{aligned} G_E &= F_1 + \frac{q^2}{4M^2}F_2 \\ G_M &= F_1 + F_2 \end{aligned}$$

$$G_E(0) = 1$$
$$G_M(0) = \mu_p \approx 2.793$$

At tree level,

$$c_D = 1 + 8G'_E(0) \equiv 1 + \frac{4}{3}r_E^2$$

Need c_D correct to $O(\alpha)$:

$$G'_E(0) \equiv \frac{1}{6}(r_E^p)^2 + \frac{\alpha}{3\pi m_p^2} \log \frac{m_p}{\lambda}$$

(or equivalent IR finite observable)

Defines r_E in presence of radiative corrections

- can extract from/compare to electronic hydrogen
  - must use *same* definition in comparison to hydrogen data (more later)
- can extract from measured electron-proton scattering data
  - Assume that two-photon exchange can be reliably subtracted (more later)
  - Need to extrapolate to $Q^2=0$ to find slope, and hence c_D

analyticity and form factor constraints

What functional form to use in extrapolating to $Q^2=0$?

$$G_E = 1 + a_1 q^2 + a_2 q^4 + \dots$$

[Simon et al 1980]

radius of convergence < 4 m_π^2

$$G_E = \frac{1}{1 + a_1 \frac{q^2}{1 + a_2 \frac{q^2}{1 + \dots}}}$$

[Sick 2003]

no control on parameters

fundamental problem: need larger Q^2 to increase statistics but then introduce sensitivity to more parameters (need even more statistics, ...)

analyticity:

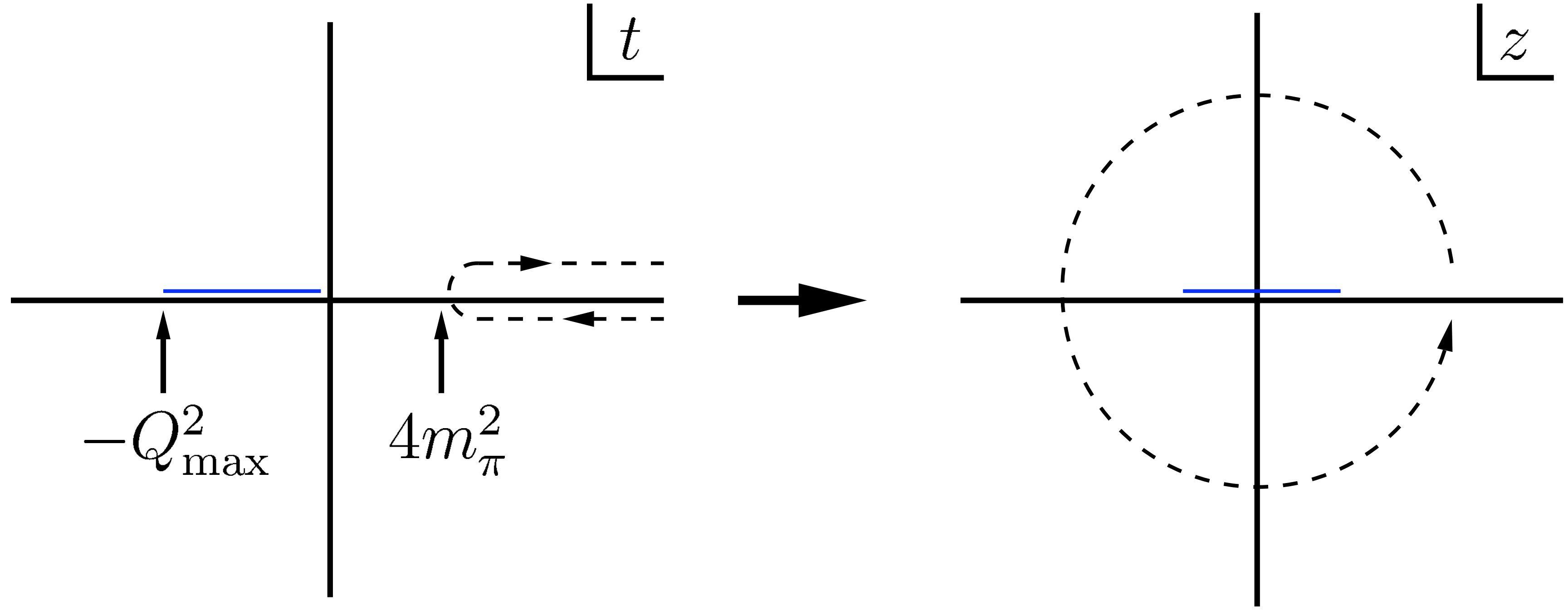

- extended to complex values of $t=q^2$, form factor is analytic outside cut in t plane

$$z(t, t_{\rm cut}, t_0) = \frac{\sqrt{t_{\rm cut} - t} - \sqrt{t_{\rm cut} - t_0}}{\sqrt{t_{\rm cut} - t} + \sqrt{t_{\rm cut} - t_0}}$$

$4m_\pi^2$ (isovector channel)

point mapping to z=0 (scheme choice)

- sums simple Taylor expansion, ensuring convergence through entire physical range

techniques familiar from meson transition form factors, e.g. B→π

[Bourrely et al 1981]
[Boyd, Grinstein, Lebed 1995]
[Lellouch et al 1996]
[Arnesen et al 2005]
[Becher, Hill 2006] ....

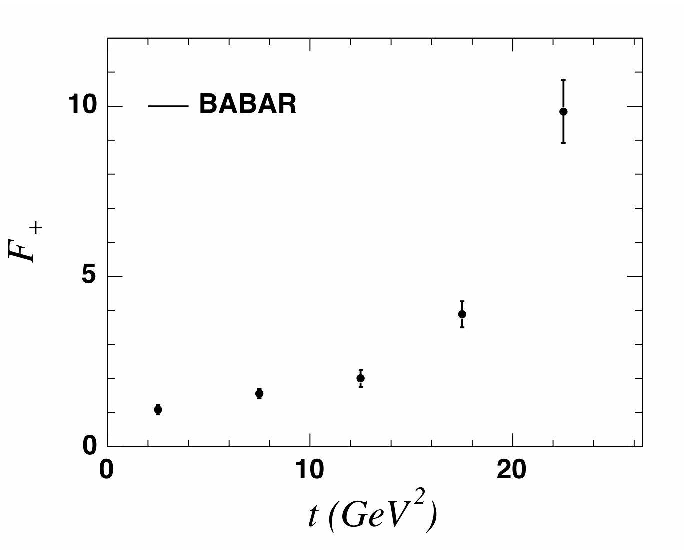

→

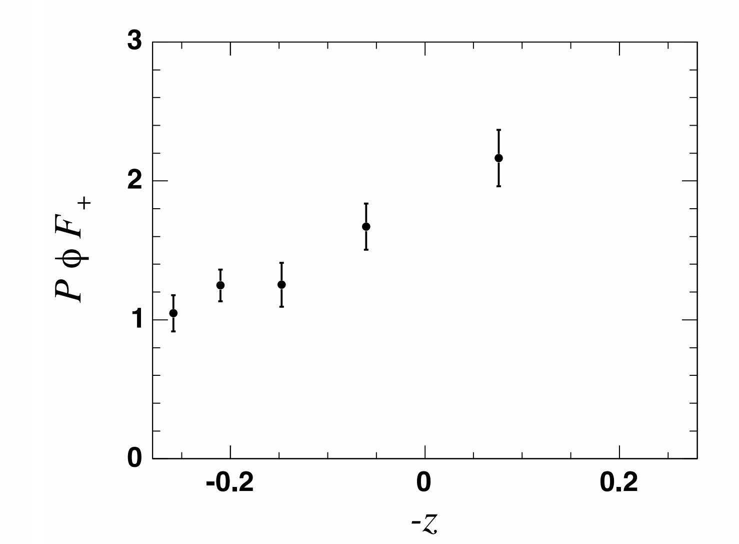

- basic idea: small expansion parameter (z), *order unity* expansion coefficients

$$G(q^2) = \sum_{n=0}^{\infty} a_n z(q^2)^n$$

- in fact, a little better, since can show

$$\sum_{n=0}^{\infty} a_n^2 < \infty \quad \Rightarrow$$

a_n *smaller* for large n

- a form factor not in this class is in violation of QCD; conversely, stronger constraints require more knowledge (that should be made explicit)

For the cognoscenti, the real power of the expansion is based on observation of O(1) coefficients, not unitarity bounds.   Example from K→π vector form factor

unitarity bound on A (require exclusive rate< inclusive rate)

$$A = \sqrt{\sum_k \frac{a_k^2}{a_0^2}}$$

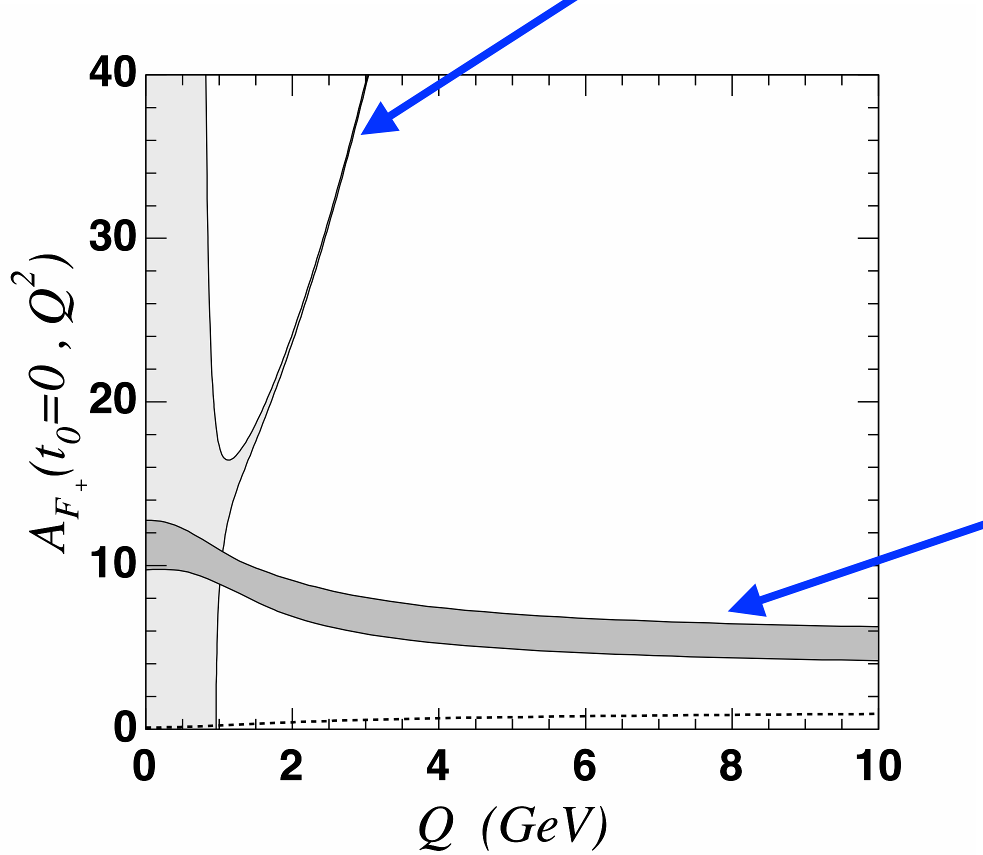

actual size of A
(measured τ→Kπν)

[RJH PRD 2006]

scheme choice to evaluate OPE for inclusive rate

⇒ Unitarity bound either uncertain (low Q) or overestimates bound (high Q)

For nucleon form factors, unitarity even less relevant, as dominant dispersive contribution to form factors is from states below NN threshold

- study of vector dominance models, ππ approximation to isovector form factors: expect O(1) is really order 1 (e.g. not 10)

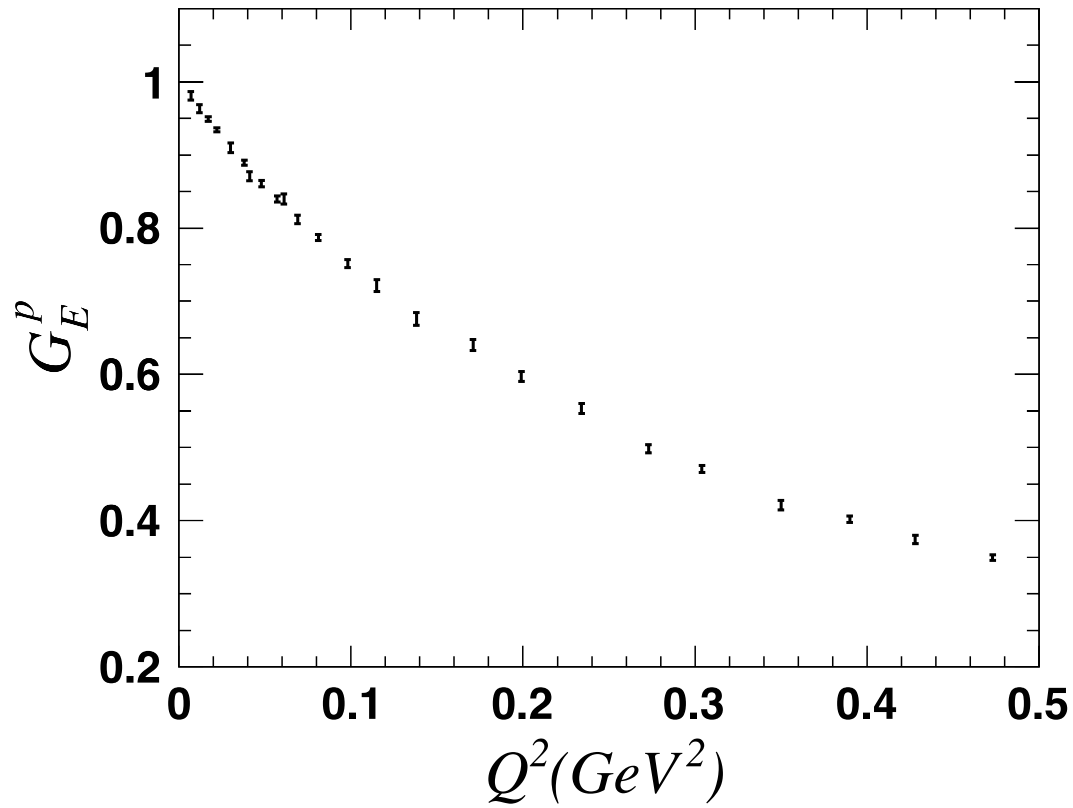

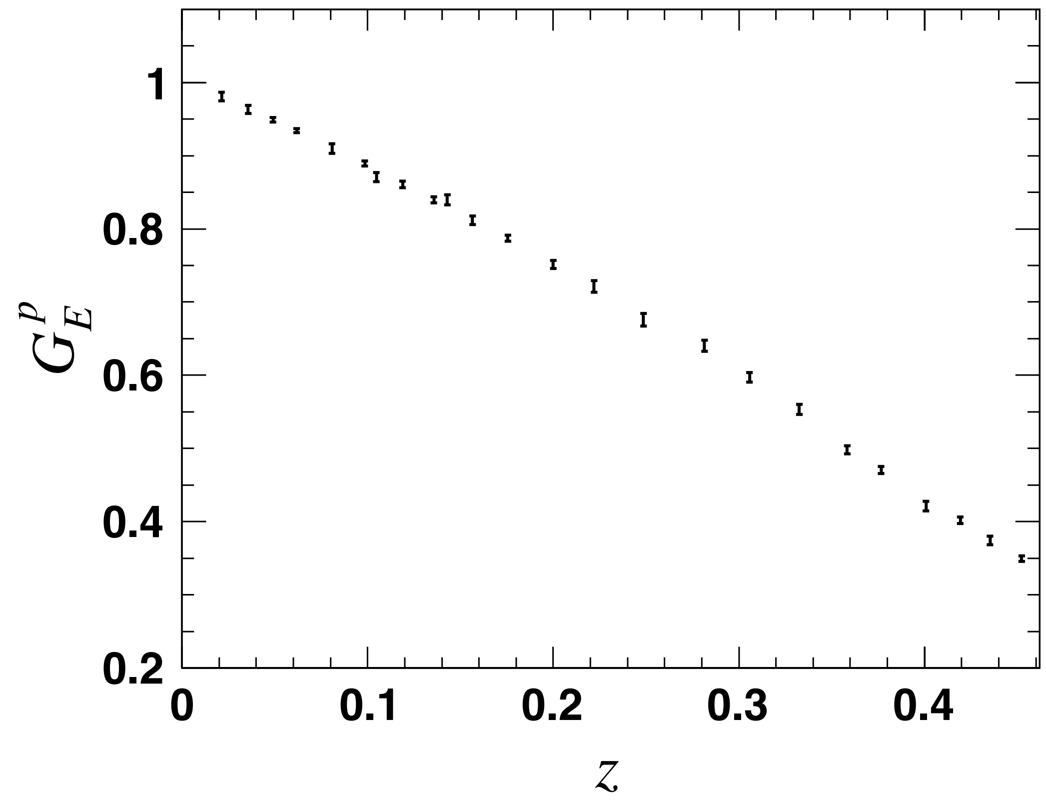

- more concretely, fits to data yield

$$a_0 \equiv 1\,, \quad a_1 = -1.01(6)\,, \quad a_2 = -1.4^{+1.1}_{-0.7}\,, \quad a_3 = 2^{+2}_{-6}$$

- to assign error, constrain coefficients <5 (conservative) or <10 (very conservative)

results: proton scattering data

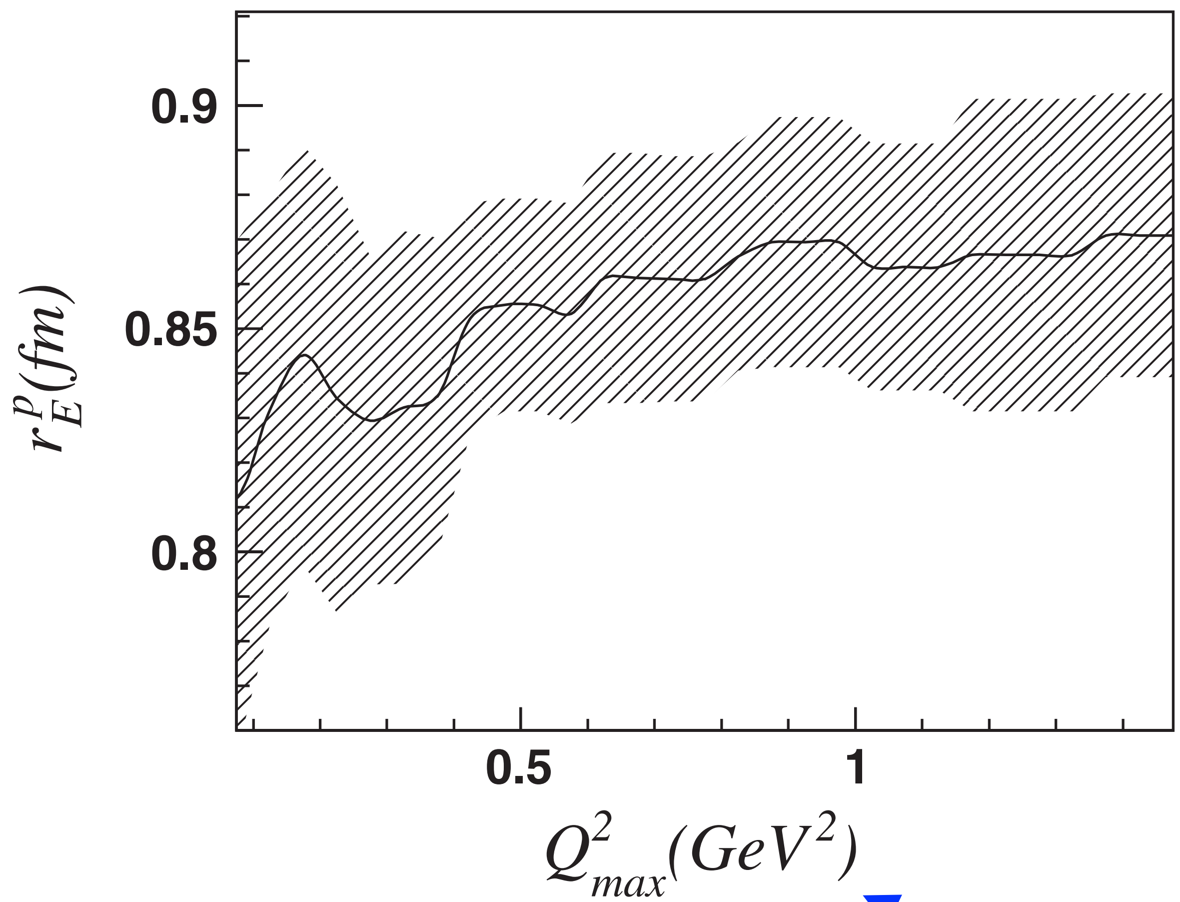

$$r_E^p = 0.870 \pm 0.023 \pm 0.012\,\mathrm{fm}$$

expt

shape: $|a|<5 \to |a|<10$

data from Arrington et al compilation PRC 2007

maximum Q^2

- larger Q^2 range: sensitive to more coefficients in expansion, but doesn't improve slope at $Q^2=0$

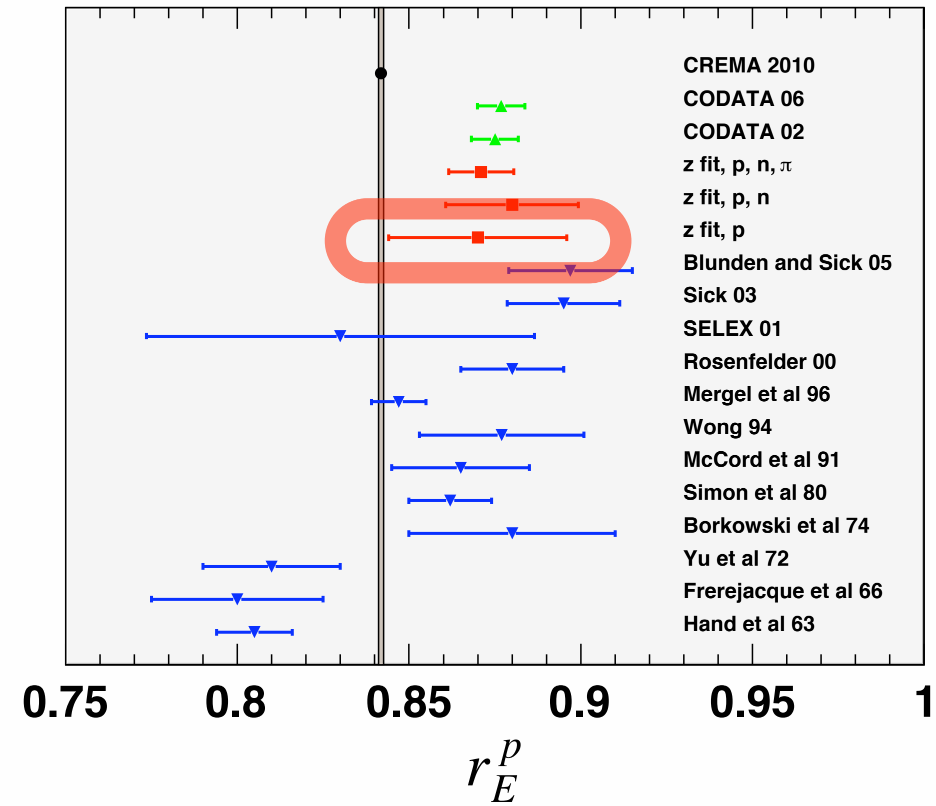

results: proton + neutron scattering data

- isoscalar threshold is actually higher ($9m_\pi^2$ vs $4\,m_\pi^2$)

- higher threshold ⇒ smaller z ⇒ stronger constraints

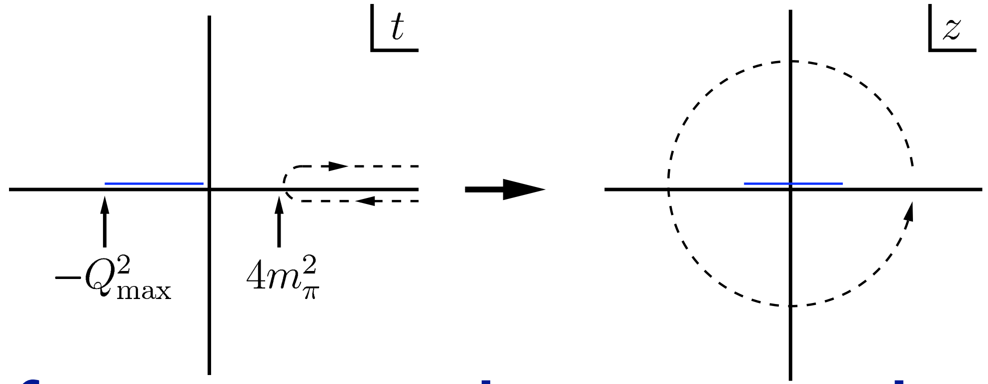

- use combined fit of proton and neutron data to decompose isoscalar and isovector

$$r_E^p = 0.880^{+0.017}_{-0.020} \pm 0.007\,\text{fm}$$

expt

shape:
$|a|<5 \to |a|<10$

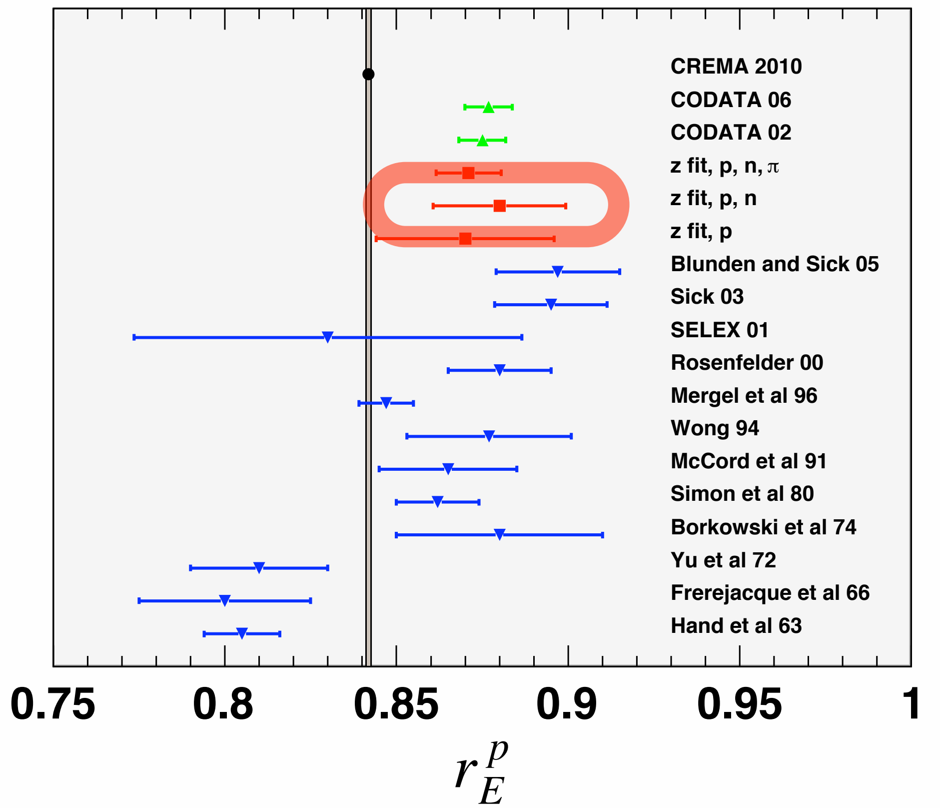

results: proton + neutron scattering data, and ππ→NÑ data

- in isovector channel, only ππ states contribute below $16m_\pi^2$

[Hohler, Pietarinen 1975]

$$\mathrm{Im}\, G_E^{(1)}(t) = \frac{2}{m_N\sqrt{t}}(t/4 - m_\pi^2)^{3/2} F_\pi(t)^* f_+^1(t),$$

pion form factor

partial amplitude for ππ→NÑ

- effectively raise the isovector threshold (⇒smaller z) by including this contribution explicitly

$$G_E^{(1)}(t) = G_{\mathrm{cut}}(t) + \sum_k a_k z^k(t, t_{\mathrm{cut}} = 16m_\pi^2, t_0)$$

results: proton + neutron scattering data, and $\pi\pi \to N\bar{N}$ data

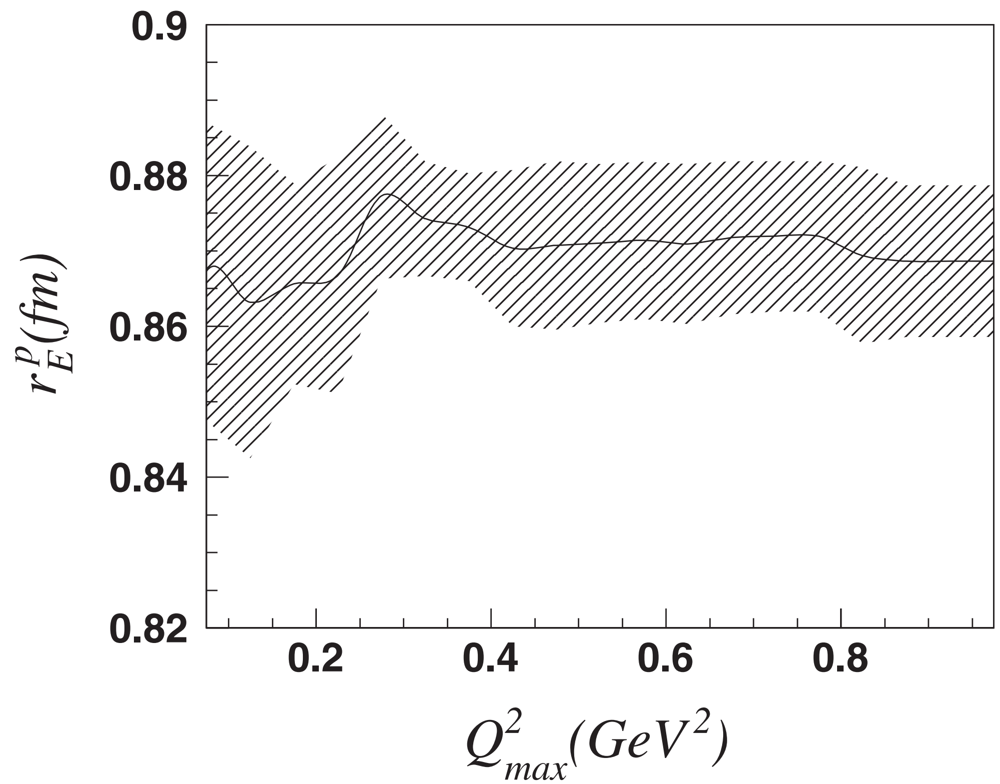

normalization error for $\pi\pi$ continuum (30%)

$$r_E^p = 0.871 \pm 0.009 \pm 0.002 \pm 0.002\,\mathrm{fm}$$

expt

shape: $|a|<5 \to |a|<10$

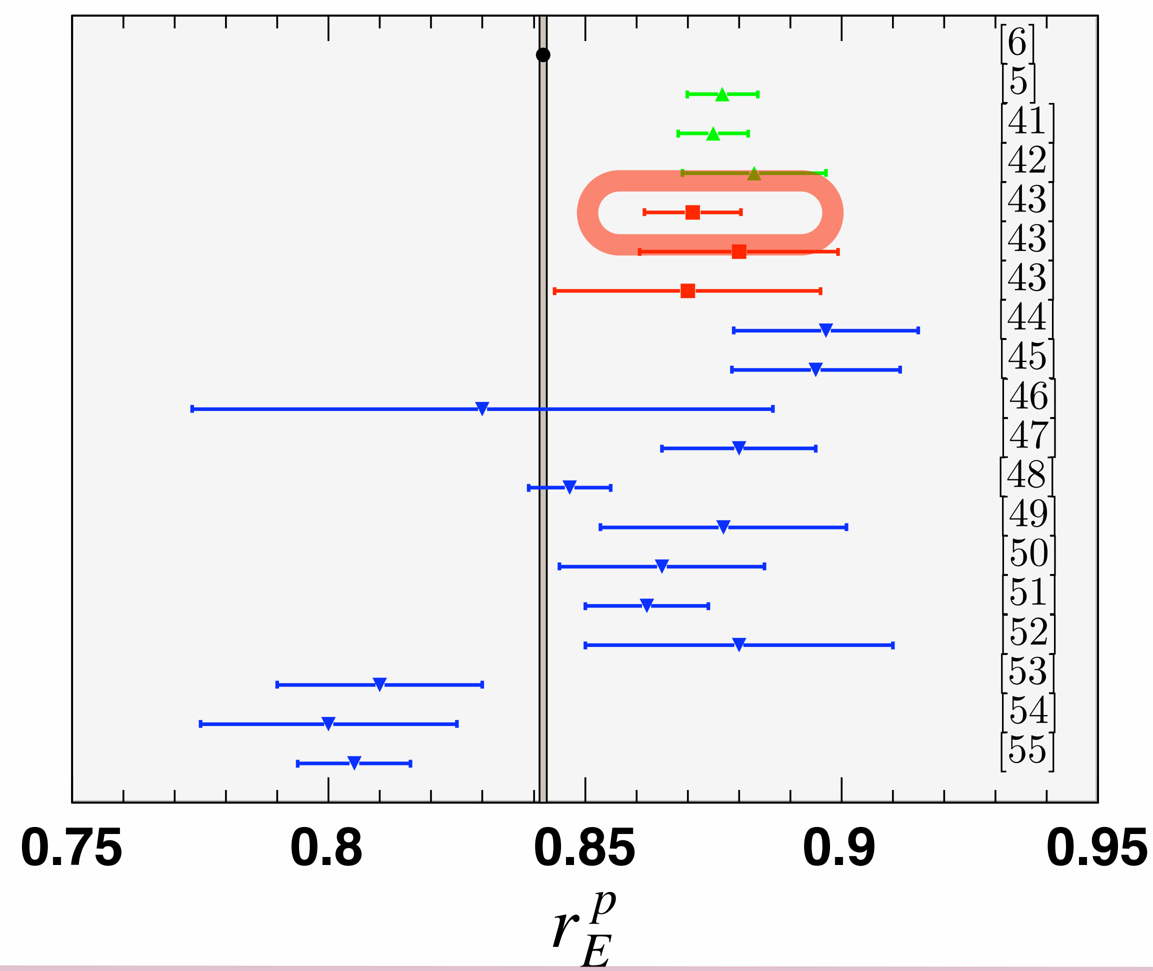

- consistent results for r_E using proton, proton+neutron, proton +neutron+$\pi\pi$, different Q^2 ranges

- leaves significant discrepancy with muonic H extraction

Investigate scheme dependence: no significant effect

TABLE III. The rms charge radius extracted using electron-proton and electron-neutron scattering data, and different schemes presented in the text. The neutron form-factor slope is constrained using (31). A cut $Q^2_{\rm max} = 0.5$ GeV^2 is enforced. In the lower part of the table, the bounds on $\sum_k a_k^2$ from Table II are multiplied by 4. $\phi_{\rm VMD}$ and $\phi_{\rm OPE}$ are defined in Eqs. (22) and (23).

	$k_{\rm max} = 2$	3	4	5	6
$\phi = 1,\ t_0 = 0,\ \lvert a_k\rvert \le 10$	888^{+5}_{-5}	865^{+11}_{-11}	888^{+17}_{-22}	882^{+21}_{-22}	878^{+20}_{-19}
	$\chi^2 = 33.67$	23.65	21.80	21.13	20.47
$\phi = 1,\ t_0 = 0,\ \lvert a_k\rvert \le 5$	888^{+5}_{-5}	865^{+11}_{-11}	881^{+10}_{-16}	885^{+16}_{-21}	882^{+18}_{-20}
	$\chi^2 = 33.67$	23.65	21.95	21.46	21.06
$\phi = \phi_{\rm VMD},\ t_0 = 0,\ \lvert a_k\rvert \le 10$	865^{+6}_{-6}	874^{+12}_{-13}	884^{+23}_{-24}	879^{+24}_{+22}	877^{+22}_{-20}
	$\chi^2 = 23.26$	22.50	22.15	21.59	21.09
$\phi = 1,\ t_0 = 0$	888^{+5}_{-5}	865^{+11}_{-11}	880^{+13}_{-16}	882^{+14}_{-18}	882^{+15}_{-18}
	$\chi^2 = 33.67$	23.65	22.07	21.45	21.18
$\phi = \phi_{\rm OPE},\ t_0 = 0$	904^{+5}_{-5}	861^{+10}_{-11}	888^{+14}_{-21}	883^{+20}_{-20}	881^{+20}_{-19}
	$\chi^2 = 61.34$	24.38	21.62	20.86	20.51
$\phi = \phi_{\rm OPE},\ t_0 = t_0^{\rm opt}(0.5\ {\rm GeV}^2)$	912^{+5}_{-5}	869^{+9}_{-9}	887^{+18}_{-19}	881^{+20}_{-19}	880^{+20}_{-19}
	$\chi^2 = 93.69$	22.54	21.05	20.32	20.32

NRQED part (2): two-photon exchange

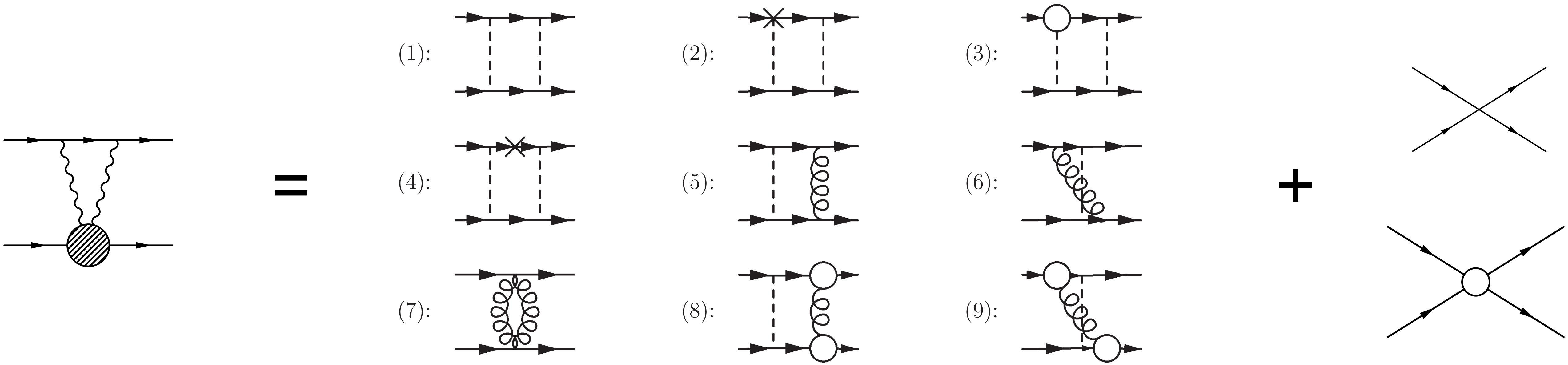

- to reproduce large momentum regions, include four-fermion counterterms

$$\mathcal{L}_{\rm ct} = \frac{d_1}{M^2}\psi_p^\dagger\psi_p\psi_e^\dagger\psi_e + \frac{d_2}{M^2}\psi_p^\dagger\vec{\sigma}\psi_p\cdot\psi_e^\dagger\vec{\sigma}\psi_e + \dots$$

- perform matching at a convenient point, e.g. all external particles onshell, at rest: hadronic part is forward Compton amplitude

forward Compton amplitude

- QCD input summarized by amplitudes of forward scattering

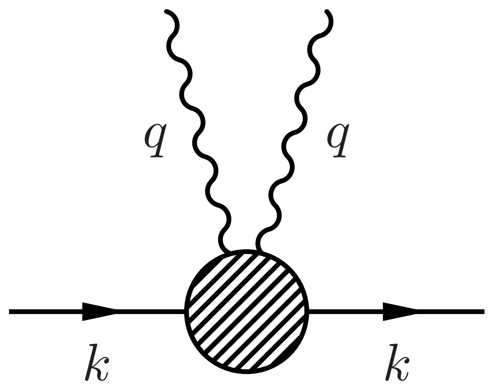

$$W^{\mu\nu}(q,k) = i\int d^4x\, e^{iq\cdot x}\langle \text{proton}(k,s)|T\{J^\mu(x)J^\nu(0)\}|\text{proton}(k,s)\rangle$$
$$= \bar{u}_s(k)\Big\{ \left(-g^{\mu\nu} + \frac{q^\mu q^\nu}{q^2}\right) W_1(\nu,Q^2) + \left(k^\mu - \frac{k\cdot q}{q^2}q^\mu\right)\left(k^\nu - \frac{k\cdot q}{q^2}q^\nu\right) W_2(\nu,Q^2)$$
$$+ H_1(\nu,Q^2)\{[\gamma_\nu,\not{q}]k_\mu - [\gamma_\mu,\not{q}]k_\nu + [\gamma_\mu,\gamma_\nu]k\cdot q\}$$
$$+ H_2(\nu,Q^2)\{[\gamma_\nu,\not{q}]q_\mu - [\gamma_\mu,\not{q}]q_\nu + [\gamma_\mu,\gamma_\nu]q^2\}\Big\} u_s(k)$$

- four invariant functions of photon energy ν and invariant Q^2: two spin-independent, two spin-dependent

- in DIS, just interested in imaginary part, but here need the whole thing

dispersion relations for forward amplitudes

$$W_2(\nu, Q^2) = \frac{1}{\pi}\int_0^\infty d\nu'^2 \frac{\mathrm{Im}W_2(\nu', Q^2)}{\nu'^2 - \nu^2} = W_2^{\mathrm{proton}}(\nu, Q^2) + \frac{1}{\pi}\int_{\nu^2_{\mathrm{cut}}}^\infty d\nu'^2 \frac{\mathrm{Im}W_2(\nu', Q^2)}{\nu'^2 - \nu^2}$$

onshell proton form factors

inelastic cross section

$\Rightarrow$ determined by measurable quantities

what if the dispersion integral doesn't converge?

$$W_1(\nu, Q^2) = W_1(0, Q^2) + \frac{\nu^2}{\pi}\int_{\nu^2_{\mathrm{cut}}}^\infty d\nu'^2 \frac{\mathrm{Im}W_1(\nu', Q^2)}{\nu'^2(\nu'^2 - \nu^2)}$$

??

DIS structure function

dispersion relation with subtraction:

- $W_1(\nu,Q^2)$ *not* determined by imaginary part

$$W_1(\nu,Q^2) = W_1(0,Q^2) + \frac{\nu^2}{\pi}\int_{\nu^2_{\rm cut}}^{\infty} d\nu'^2 \frac{{\rm Im}W_1(\nu',Q^2)}{\nu'^2(\nu'^2-\nu^2)}$$

- no intrinsic meaning to "proton contribution" and "non-proton contribution" to $W_1(0,Q^2)$

- can analyze at low momentum using NRQED: double scattering of proton off external static electromagnetic field

having determined the Wilson coefficients from data, find the leading behavior of $W_1(0,Q^2)$ at small Q^2:

$$\begin{aligned} W_1(0,Q^2) &= 2(-1+{c_F}^2) + \frac{Q^2}{2M^2}\left({c_F}^2 - 2c_F c_{W1} + 2c_M + c_{A1}\right) + \dots \\ &= 2a_p(2+a_p) + \frac{Q^2}{2M^2}\left(-8a_p F_1'(0) - 8(1+a_p)F_2'(0) + M^3\frac{4\pi}{e^2}\bar\beta\right) + \dots \\ &\approx 14 + \frac{Q^2}{\mathrm{GeV}^2}(-78+6) + \dots \end{aligned}$$

OPE expansion at large Q^2:

$$W_1(0,Q^2) \approx \frac{4M^2}{Q^2}\sum_f e_f^2\left(A_f^{(2)} - f_{T_f}\right)$$

$$\langle P(\boldsymbol{k})|\bar q_f\left(\gamma^{\{\mu}iD^{\nu\}} - \frac14 g^{\mu\nu} i\not{D}\right)q_f|P(\boldsymbol{k})\rangle \equiv 2A_f^{(2)}\left(k^\mu k^\nu - \frac14 g^{\mu\nu}M^2\right)$$

$$\langle P(\boldsymbol{k})|m_f\bar q_f q_f|P(\boldsymbol{k})\rangle \equiv 2M^2 f_{T_f}$$

How do we interpolate ?

Previous analyses use ansatz of "proton" + "non-proton"

$$
\begin{aligned}
W_1(0,Q^2) &= 2(-1+{c_F}^2) + \frac{Q^2}{2M^2}\left({c_F}^2 - 2c_F c_{W1} + 2c_M + c_{A1}\right) + \dots \\
&= \underbrace{2a_p(2+a_p) + \frac{Q^2}{2M^2}\left(-8a_p F_1'(0) - 8(1+a_p)F_2'(0)\right.}_{2F_2(-Q^2)[2F_1(-Q^2)+F_2(-Q^2)]} + \left.\underbrace{M^3\frac{4\pi}{e^2}\bar\beta}_{\frac{4\pi}{e^2}\bar\beta\frac{MQ^2}{2}\frac{1}{\left(1+Q^2/0.71\,\mathrm{GeV}^2\right)^4}}\right) + \dots
\end{aligned}
$$

e.g. Pachucki 1999

- assumes ad hoc separation into "proton" versus "non-proton" states, and assigns form factors to the former

- wrong behavior at large Q^2 ($1/Q^6$ instead of $1/Q^2$)

This ansatz fails dramatically for experimentally accessible spin-dependent structure function

$$\Gamma_1 = \frac{Q^2}{8}\bar{S}_1 = \frac{MQ^2}{4}\bar{H}_1$$

~ 0.8 GeV^{-2}

Drell Hearn

$$S_1(0,Q^2) - S_1^{\rm proton}(0,Q^2) = -\frac{1}{M}a_p^2 + cQ^2 + \dots$$
$$= \frac{1}{\pi}\int d\nu^2 \frac{{\rm Im}S_1(\nu,Q^2)}{\nu^2}$$

data (unsubtracted dispersion relation)

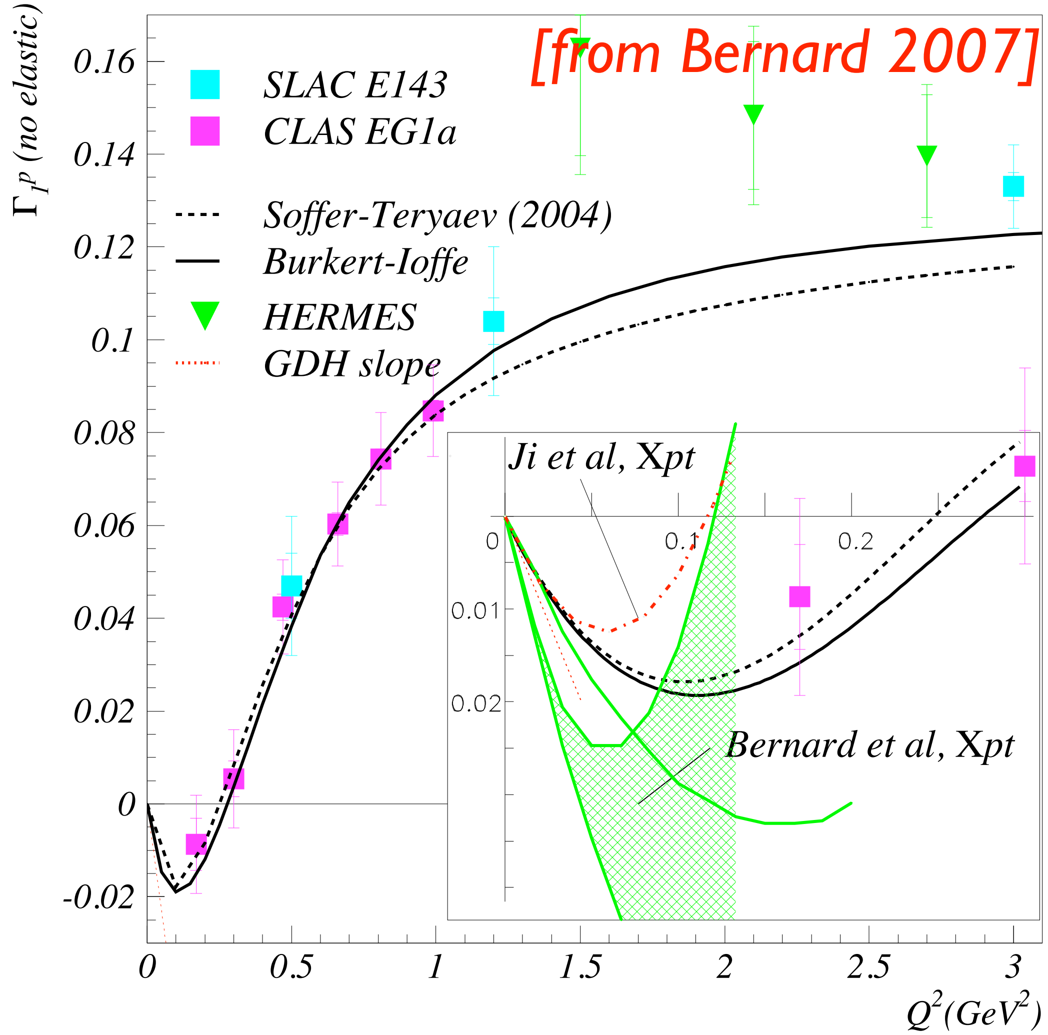

This ansatz fails dramatically for experimentally accessible spin-dependent structure function

$$\Gamma_1 = \frac{Q^2}{8}\bar{S}_1 = \frac{MQ^2}{4}\bar{H}_1$$

~ 0.8 GeV^{-2}

Drell Hearn

$$S_1(0,Q^2) - S_1^{\rm proton}(0,Q^2) = -\frac{1}{M}a_p^2 + cQ^2 + \dots$$
$$= \frac{1}{\pi}\int d\nu^2 \frac{{\rm Im}S_1(\nu,Q^2)}{\nu^2}$$

data (unsubtracted dispersion relation)

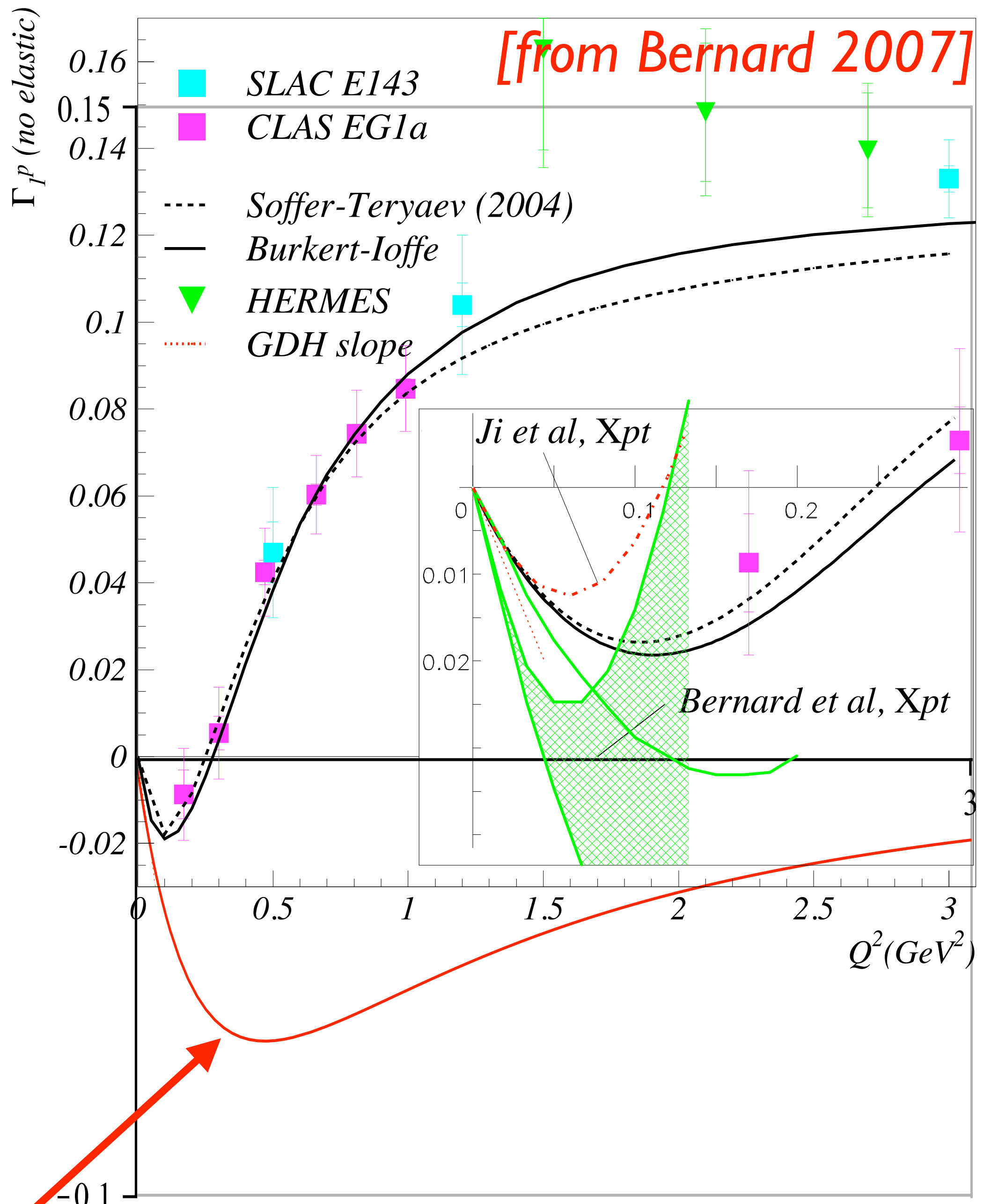

SIFF (sticking in form factors) ansatz

- model independently, in small lepton mass limit, 2-photon contribution to energy is

$$\Delta E(nS) = (Z\alpha)^5 \frac{m_r^3}{\pi n^3} \frac{m_e}{m_p} \left\{ \log m_e \left[m_p^3 \frac{4\pi}{e^2} \left(5\bar{\alpha} - \bar{\beta}\right) - 3a_p^2 \right] + c_0 + c_1 m_e + \dots \right\}$$

universal hadronic parameters

- unfortunately, m_μ/m_π , $m_\mu/(m_\Delta - m_p)$ not small

Note that low energy μp scattering, including radiative corrections, is predicted by NRQED: sufficient data can determine d_2

- proposal for μ^+p, μ^-p scattering (PSI, Gilman, Piasetzky et al)
- systematic computations in progress

In absence of a measurement for this new hadronic quantity, uncertainty of ~0.004 meV is not justified

		[Pachucki]	*[Borie]*	*[Hill, Paz]*	
Contribution		Ref. [20]	Ref. [23]	This work	
δE^{vertex}		-0.0099	-0.0096	-0.0108	
$\delta E^{\text{two}-\gamma}$	$\delta E_{\mu H}^{\text{proton}}$	0.035	0.051	-0.016	
	$\delta E_{\mu H}^{W_1(0,Q^2)}$			Model Dependent	
	$\delta E_{\mu H}^{\text{continuum}}$			0.013 [19]	*[Carlson, Vanderhaegen]*
Total		0.025	0.042		

TABLE I: Comparison between this and previous works for $\mathcal{O}(\alpha^5)$ proton structure corrections to the $2P-2S$ Lamb shift in muonic hydrogen, in meV.

Investigate the impact of modified structure corrections and larger uncertainty on the two-photon exchange contribution

	Pohl et al compilation (Nature 2010)	RJH, Paz	reason for change
vertex correction	-0.0096 meV	-0.0108	mismatch in r definitions
two photon (d_2)	0.051	? ~ 0.05 +/- 0.05	model dependent
"recoil finite size"	0.013	0	double counting
total	210.0011(45) $-5.2262r^2$	209.987(50) $-5.2262\, r^2$	
extracted radius	0.8421(6) fm	0.841(6) fm	

H	CODATA06	0.876(8)	4.2σ	3.5σ
e-p	Sick 2005	0.895(18)	2.9σ	2.8σ
	JLab 2011	0.875(10)	3.3σ	2.9σ
	Mainz	0.879(8)	4.6σ	3.8σ
H and e-p	CODATA10	0.8775(51)	6.9σ	4.6σ
	ep	0.870(26)	1.1σ	1.1σ
	ep, en	0.880(20)	1.9σ	1.9σ
	ep, en, ppNN	0.871(10)	2.9σ	2.6σ

Summary

The proton radius is still a puzzle.

- most mundane resolution may be ~5σ shift in Rydberg (less mundane resolutions postulated)

- z expansion provides model independent extrapolation for radius determination from scattering data
  - analysis should/will be implemented with most recent scattering data
  - NRQED can be used to eliminate model dependence in radiative corrections at low energy

- NRQED analysis of proton structure for hydrogenic bound states
  - model independent translation between scattering and bound state observables
  - model-dependent assumptions in previous analyses
  - possibility of significant new effects in contact interaction describing two-photon exchange
  - can measure strength of this contact interaction directly in muon-proton scattering

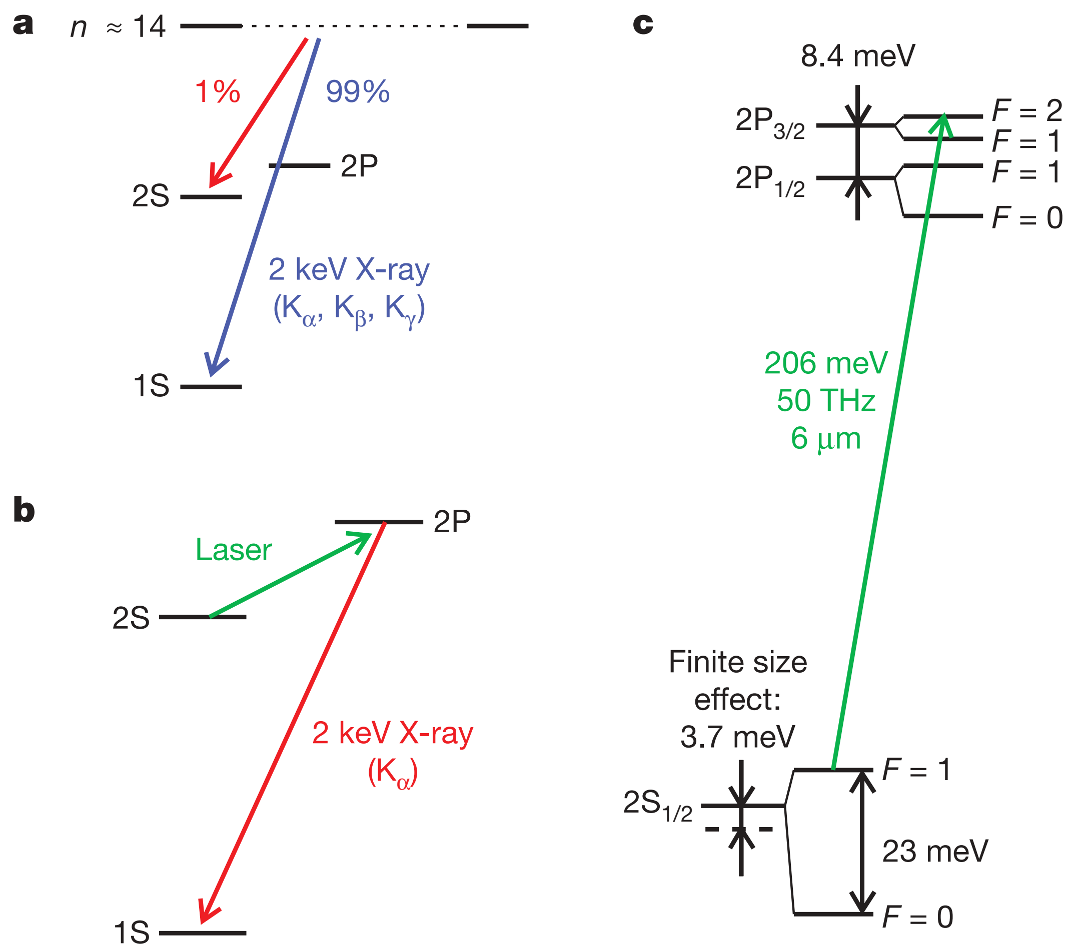

Figure 1 | Energy levels, cascade and experimental principle in muonic hydrogen. **a**, About 99% of the muons proceed directly to the 1S ground state during the muonic cascade, emitting 'prompt' K-series X-rays (blue). 1% remain in the metastable 2S state (red). **b**, The μp(2S) atoms are illuminated by a laser pulse (green) at 'delayed' times. If the laser is on resonance, delayed K_α X-rays are observed (red). **c**, Vacuum polarization dominates the Lamb shift in μp. The proton's finite size effect on the 2S state is large. The green arrow indicates the observed laser transition at $\lambda = 6$ µm.

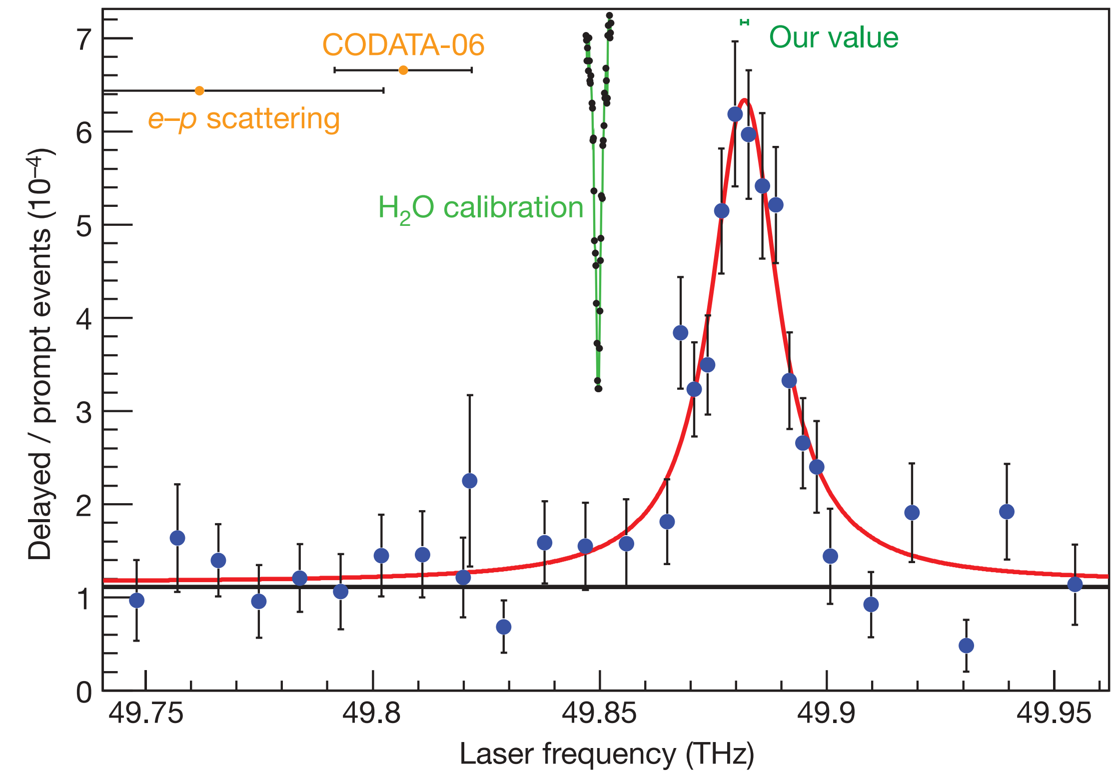

Figure 5 | Resonance. Filled blue circles, number of events in the laser time window normalized to the number of 'prompt' events as a function of the laser frequency. The fit (red) is a Lorentzian on top of a flat background, and gives a χ^2/d.f. of 28.1/28. The predictions for the line position using the proton radius from CODATA[3] or electron scattering[1,2] are indicated (yellow data points, top left). Our result is also shown ('our value'). All error bars are the ±1 s.d. regions. One of the calibration measurements using water absorption is also shown (black filled circles, green line).

Aside: similar analysis for axial radius of relevance to neutrino scattering

[data from MiniBooNE, PRD81, 092005 (2010)]

dipole model
model-indep.

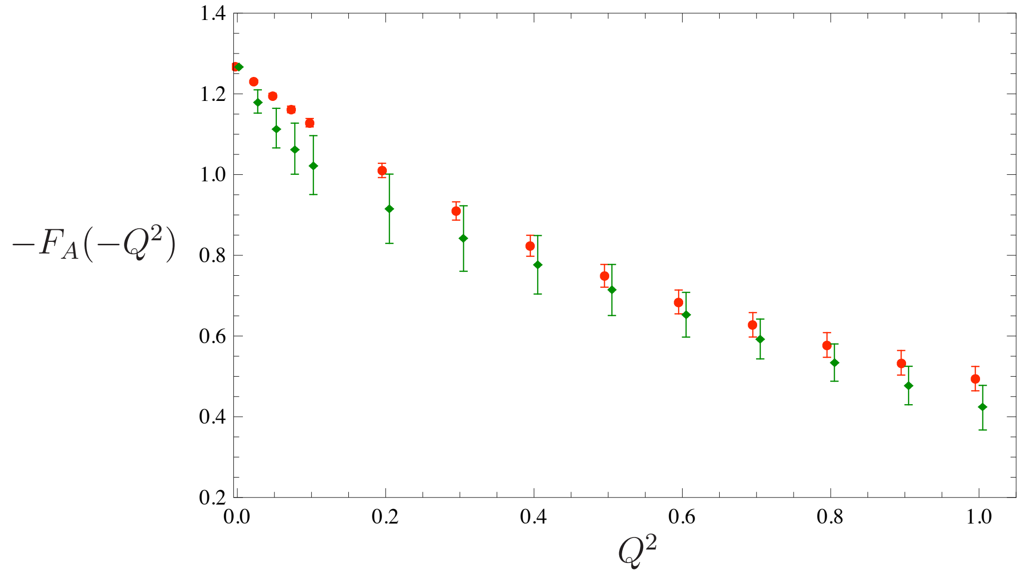

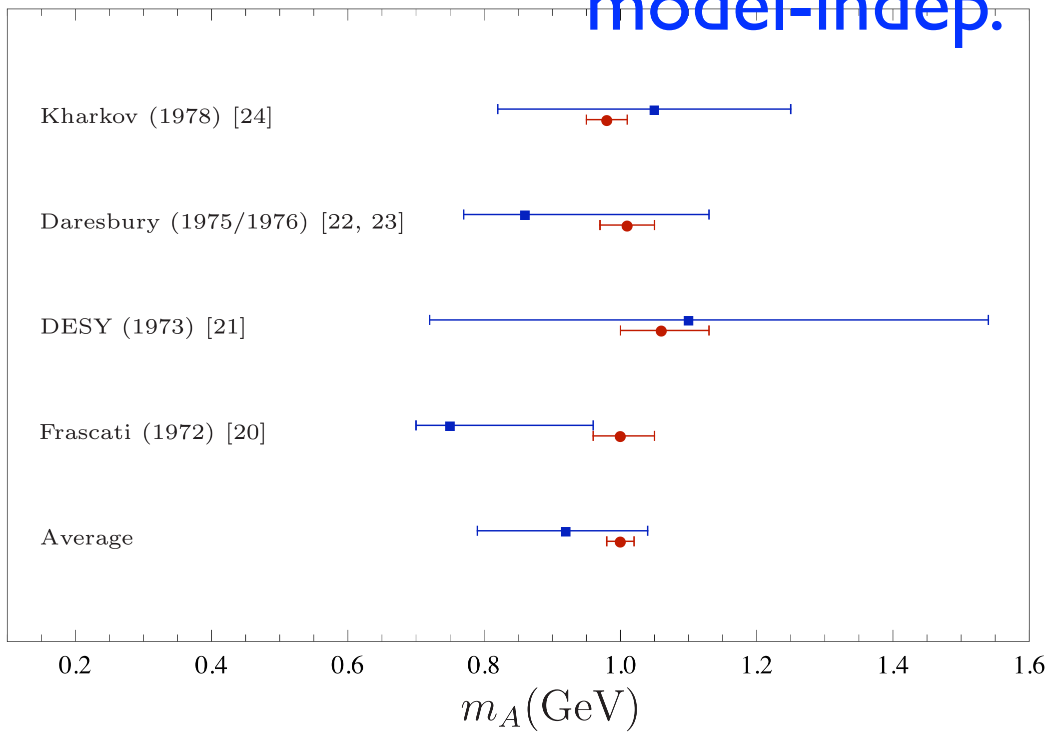

$$\boxed{m_A = 0.85^{+0.22}_{-0.07} \pm 0.09\,\mathrm{GeV} \qquad \text{(neutrino scattering)}}$$

$$\boxed{m_A = 0.92^{+0.12}_{-0.13} \pm 0.08\,\mathrm{GeV} \qquad \text{(electroproduction)}}$$

$$m_A^{\mathrm{dipole}} = 1.29 \pm 0.05\,\mathrm{GeV}$$

$$m_A^{\mathrm{dipole}} = 1.00 \pm 0.02\,\mathrm{GeV}$$

$$r_A = \begin{cases} 0.80^{+0.07}_{-0.17} \pm 0.12\,\mathrm{fm} & \text{(neutrino scattering)} \\ 0.74^{+0.12}_{-0.09} \pm 0.05\,\mathrm{fm} & \text{(electroproduction)} \end{cases}$$

Using default nuclear model (relativistic fermi gas), discrepancy can be attributed to incorrect form factor assumption